Experimental post-entrapment water loss from synthetic CO₂-H₂O inclusions in natural quartz

RONALD J. BAKKER and J. BEN H. JANSEN

Department of Geochemistry, Institute for Earth Sciences, University of Utrecht, PO Box 80.021, 3508 TA Utrecht, The Netherlands

Abstract—Artificial fluid inclusions were hydrothermally synthesized by crack healing in natural Brazilian quartz. Two original experiments E421 and E679 with a H_2O-CO_2 fluid were carried out at 835 K, 200 MPa, over 38 days, and at 856 K, 211 MPa, over 35 days, respectively. In both experiments homogeneous three-phase (a vapor and two liquids) fluid inclusions were synthesized with 22 and 20 mol% CO_2, respectively. The CO_2 phases homogenize to the vapor phase at 302.2 ± 0.1 K (E679, cores 1 and 2), and to the liquid phase at 303.6 ± 0.3 K (E421, core 3), 303.9 ± 0.2 K (E421, core 4). The CO_2-H_2O phases homogenize to the vapor phase at 573.6 ± 0.4 K (E679, core 1 and 2), 575.6 ± 1.5 K (E421, core 3), and 576.1 ± 0.8 K (E421, core 4). Micro cracks and the new hydrothermally precipitated quartz, which directly surrounds the inclusions, were studied with TEM and SEM. The healed cracks have numerous growth imperfections that provide many possible routes for fluid transport. Dislocation arrays and small channels were observed and are often connected to the inclusions.

Quartz cores 3 and 4 were subsequently re-equilibrated for 21 and 27 days respectively under hydrothermal conditions with pure H_2O, at both a lower pressure of 100 MPa (E463) and a higher pressure of 365 MPa (E490) than that of the original experiment E421. The temperatures of the re-equilibration experiments were equal to the original (835 K). In E463, the internally overpressured re-equilibration, only traces of solution and precipitation of quartz were evident with minor transformation of the angular walls to more rounded forms. Volume increase for some inclusions resulted from decrepitation. The homogenization of the CO_2-H_2O phases to the gas phase occurred at higher temperatures, up to 604 K. In E490, the internally underpressured re-equilibration, major solution and precipitation resulted in the transformation of irregular shaped inclusion walls and formation of secondary inclusions halos. The homogenization of the CO_2-H_2O phases to the gas phase occurred at lower temperatures, down to 565 K. The fluids in inclusions from both re-equilibration experiments were found to have lower densities than the original fluids synthesized. This is quantified by the increased volumetric proportions of CO_2 vapor. The CO_2 fraction in inclusions was found to have increased, by up to 54 mol%. The change in homogenization temperatures and the decrease in the proportions of H_2O in the original inclusions favours a model in which preferential transport of H_2O occurs along mobile dislocation lines, small intercrystalline nanocracks, and/or channels.

Results from experiment V1 and V4, using cores 1 and 2, indicate that the changes observed in the re-equilibration experiments are not artifacts of the experimental method.

INTRODUCTION

NON-LEAKAGE BEHAVIOUR of fluid inclusions (fi.s) may be expected if the postmetamorphic cooling path approximately follows the isochore of an enclosed fluid mixture. However, leakage may occur if pressure-gradients exist between the fi.s and the external pore fluid. Discrepancies exist between the density and composition of fluids observed from natural inclusions and theoretical fluids calculated using metamorphic conditions deduced from geothermobarometry based on mineral equilibria.

SWANENBERG (1980) questioned whether or not inclusions acted as closed systems in natural granulites from Rogaland, southwestern Norway, where an isobaric cooling succeeded the Proterozoic granulite facies metamorphism. Water leakage was assumed for amphibolite facies quartz lenses from Naxos, Greece (JANSEN et al., 1989), where an isothermal decompression of about 300 MPa occurred as a result of rapid uplifts and associated deformation during Alpine metamorphism (JANSEN et al., 1977, ANDRIESSEN, 1978; BUICK and HOLLAND, 1989).

The role of deformation on density and compositional changes occurring in fi.s in quartz has been emphasized by KERRICH (1976), WILKINS and BARKAS (1978), URAI et al. (1989), and HOLLISTER (1989). HOLLISTER (1988) has reviewed fi.s, found in greenschist-, amphibolite-, and granulite-facies metamorphic rocks. He discusses fi.s which are assumed to have formed in the presence of a H_2O-rich phase and subsequently became CO_2-rich, due to preferential water leakage.

In the experimental work of PECHER (1981), GRATIER (1982), PECHER and BOUILLIER (1984), GRATIER and JENATON (1984), STERNER and BODNAR (1989), and BOULLIER et al. (1989), models for density changes are presented. However, they do not consider compositional changes. Two mechanisms are recognized for density changes from internal over- and underpressure: (1) volume changes by decrepitation of fi.s or plastic deformation of adjacent quartz and (2) water-loss by diffusion of OH and by hydration of the adjacent rim of the host quartz, resulting in near-constant volume. HALL et al. (1989) reported compositional changes in synthetic H_2O-CO_2 fi.s, in which methane was formed after reduction of CO_2 by the inward diffusion of H_2. Compositional changes

in synthetic H_2O-CO_2 inclusions, caused by the outward diffusion of H_2O, have been observed in both internal over- and underpressure experiments by BAKKER and JANSEN (1989, 1990).

In this paper we consider changes to both bulk density and composition of synthetic H_2O-CO_2 fi.s within natural Brazilian quartz during experiments simulating isothermal compression and isothermal decompression, in addition to isobaric cooling described by BAKKER and JANSEN (1990). The morphology of the initial cracks as well as quartz growth in healed cracks were investigated with TEM and SEM techniques in order to discover routes of leakage.

EXPERIMENTAL METHOD

Six cylindrical cores (2 mm length and 4 mm diameter) were drilled from an inclusion-free Brazilian quartz crystal, parallel to the c-axis. These were polished top and bottom. Cracks were created in these cores by rapid quenching in cold distilled water after heating to 623 K, according to the method of STERNER and BODNAR (1984). The cracks were dried as thoroughly as possible, in a vacuum line for 48 h at 573 K. In experiment E679, quartz cores 1 and 2 were put in a gold tube, one end of which had been sealed by arc welding, with 31.0 mg silver-oxalate and 18.5 mg H_2O, yielding X_{CO_2} = 16.6 ± 0.1 mol%. In experiment E421, quartz cores 3, 4, 5, and 6 were put in another gold tube, also previously sealed at one end, with 26.8 mg silver-oxalate and 14.7 mg H_2O, yielding X_{CO_2} = 17.8 ± 0.2 mol%. Subsequently, the tops of the 30 mm long capsules were arc-welded. The fi.s synthesis was performed in 75 mm diameter Tuttle-type pressure vessels, with an argon pressure medium for experiments E421, E463, E490, E679 and with a water pressure medium for experiments V1 and V4. The original experiments E421 and E679 (Table 1 and Fig. 1) were carried out at 200 MPa, 835 K and 211 MPa, 856 K, respectively. The runs were first brought to the desired pressure at room temperature (Fig. 1), the temperature was then increased, while the pressure was adjusted in several steps, until experimental conditions were reached. After the experiments the vessels were cooled to room temperature (293 K) within 30 min with an external air flow before the pressure was released.

A Fluid Inc. adapted USGS gas flow heating-freezing stage, cali-

brated using the fusion temperatures of pure H_2O, CO_2, and $NaNO_3$, was used to measure the homogenization temperatures (T_H) of the phases in the synthetic fi.s. Inclusions were optically photographed to characterize their morphology and volume percentages of the gas species (Table 2). Volume percentages were calculated by correcting the measured surface areas. The best volume estimates are achieved in flat inclusions. The mole fractions of the components (Table 2) were calculated by considering the density of each phase (H_2O liquid, CO_2 liquid and vapor) and their volume percentages. These were corrected using solubility data of CO_2 in H_2O (DODDS et al., 1956; WEAST, 1975). A Microdil-28 Raman microspectrometer with a multichannel detector (BURKE and LUSTENHOUWER, 1987) was used to check for the presence of gas species other than CO_2 in selected fi.s from both the original and re-equilibration experiments.

The experimental technique was first tested, using core 1 and 2 from synthesis run E679. This was necessary to ensure that the observations from the re-equilibration experiments were not an artifact of the experimental technique. In re-equilibration experiment V1 (Table 1), core 1 was only pressurized to 196.5 MPa at room temperature for 2 h. Experiment V4 (Table 1), using core 2, was run at 213.5 MPa and 856 K, approaching the original conditions.

In the re-equilibration study, two experiments were performed (Table 1 and Fig. 1) to simulate the effects of isothermal decompression (E463) at 100 MPa, 835 K, and isothermal compression (E490) at 365 MPa, 835 K. Well-characterised cores 3 and 4 from synthesis experiment E421 were enclosed in capsules with 10 mg pure H_2O (1) to prevent crushing or microcracking during further experimentation, due to the small non-hydrostatic pressure from the capsule walls on the cores and (2) to make a clear compositional distinction between the new (type 1 fi.s) and old generation (type 2 fi.s) inclusions. This amount of water is sufficient to maintain hydrostatic conditions in the capsules for the re-equilibration experiments, covering the total surface of the quartz cores, including any irregularities. The identical fi.s, photographed after the original experiment, were re-photographed and carefully investigated three-dimensionally using a U-stage. Their T_H values were also remeasured.

In core 5 from E421, defect structures of the quartz directly adjacent to the fi.s within the healed cracks were examined with TEM. The specimens were prepared by ion-bombardment from 15 μm thin sections and examined in a JEM-200 electron microscope operating at 200 kV.

Before experiment E421, the surface morphologies of cracks in core 6 were investigated with SEM. After E421, newly grown quartz

Table 1.

Experimental conditions, starting materials and duration of the original and re-equilibration experiments.

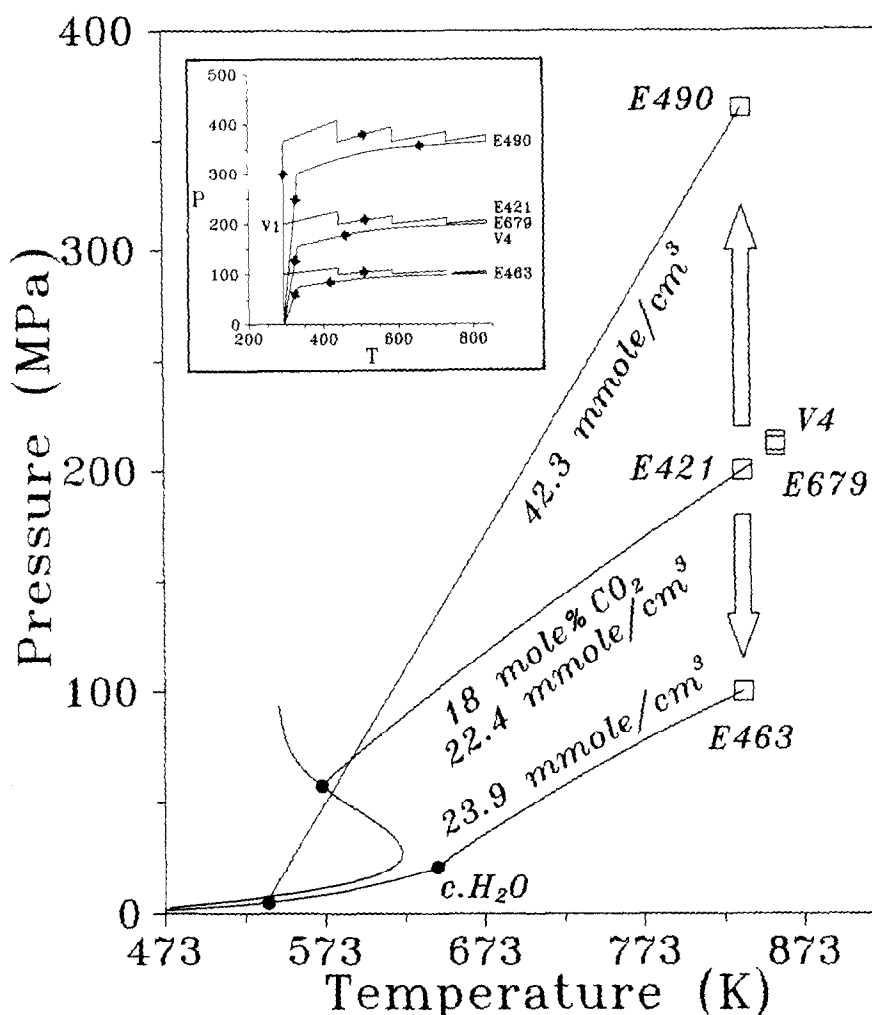| exp. number	core	pressure MPa	temperature K	mg of substances		duration
				silver-oxalate ($Ag_2C_2O_4$)	H_2O	
original synthesis experiments						
E 679	1,2	211	856	31.0	18.5	35 days
E 421	3,4,5,6	200	835	26.8	14.7	38 days
re-equilibration experiments						
V 1	1	196.5	293.2	0.0	40.0	2 hours
V 4	2	213.5	855.8	0.0	60.0	23 days
E 463	3	100	835	0.0	10.0	27 days
E 490	4	365	835	0.0	10.0	21 days

FIG. 1. *P-T* diagram for the fluids in the capsule surrounding the quartz core. The experimental conditions for E421, E679, E463, E490, and V4, and the corresponding isochores, calculated with the equation of state by CHRISTOFORAKIS and FRANCK (1986) are plotted. An 18 mol% CO_2 gas mixture isochore is indicated for E421 and E679. A pure H_2O fluid isochore is indicated for E463 and E490. The 18 mol% CO_2 miscibility gap and the boiling curve of pure H_2O are projected as curved lines. The critical point of H_2O is indicated by c.H_2O. The isothermal decompression and compression, which has a similar effect on fluid densities as isobaric cooling, are indicated with the large vertical arrows. The intersection of the isochores and the miscibility gap or the boiling curve predict the T_H of original fi.s in E421, E679, and of type 1 fi.s in E463 and E490. The schematic diagram in the upper left shows the starting and cooling *PT*-path followed by the experiments. The small arrows indicate the direction of the path.

on cracks and fi.s walls was photographed with SEM. The specimens were subsequently coated with carbon and gold for examination with a CAMSCAN electron microscope.

RESULTS

Initial Synthetic Fluid Inclusions from E421 and E679

Homogeneous generations of synthetic three-phase fi.s, containing CO_2-vapor, CO_2-liquid, and H_2O-liquid, were created in the quartz cores of the synthesis experiments E421 and E679.

In E679, cores 1 and 2 homogenize to the gas phase at the average temperature of 302.2 ± 0.1 K for vapor and liquid CO_2. The H_2O and CO_2 phases homogenize to the gas phase at average temperature of 573.6 ± 0.4 K (Table 3).

In E421, vapor and liquid CO_2 homogenize to the liquid phase at the average value 303.6 ± 0.3 and 303.9 ± 0.2 K

for core 3 and 4, respectively (Table 2 and Fig. 2). The H_2O and CO_2 phases homogenize to the gas phase at average temperatures of 575.6 ± 1.5 and 576.1 ± 0.8 K for core 3 and 4, respectively (Table 2 and Fig. 3). The average mole-fractions of CO_2 for all fi.s were calculated as 19 ± 3% for core 3, later used for E463, and 21 ± 2% for core 4, later used for E490 (Table 2).

Transmission and Scanning Electron Microscopy from E421

The newly grown quartz, directly adjacent to the synthetic fi.s in the healed crack of core 5 from E421, was examined with TEM. Most of the inclusions, which appear to be isolated by normal optical microscopy, end in long narrow channels with a maximum diameter of 0.1 μm (Fig. 4). The channels are positioned oblique or parallel to the crack surface. Many

Table 2.

Ranges, averages and standard deviations of volume estimations and mole percentage
calculations of all and flat fi.s in quartz cores 3 and 4 after the initial experiment E421,
re-used for experiment E463 and E490. Homogenization temperatures (in Kelvin) of CO_2 and CO_2-
H_2O gas mixtures are only indicated for all fi.s.

			all fi.s		flat fi.s	
			range	average	range	average
core 3	volume%	$CO_2(v)$	11.2-19.5	17 ± 2	16.3-19.5	18 ± 1
		$CO_2(l)$	20.5-35.6	30 ± 5	29.7-35.6	33 ± 3
		$H_2O(l)$	44.9-68.3	53 ± 7	44.9-54.0	49 ± 4
	mole% CO_2		11.9-24.3	19 ± 3	18.7-24.3	22 ± 2
	T_H (CO_2) to liquid		303.2-304.1	303.6 ± 0.3		
	T_H (CO_2-H_2O) to gas		573.0-578.3	575.6 ± 1.5		
core 4	volume%	$CO_2(v)$	14.7-22.1	19 ± 2	16.9-19.7	18 ± 1
		$CO_2(l)$	23.8-35.8	32 ± 3	27.4-31.9	30 ± 2
		$H_2O(l)$	42.1-61.6	49 ± 5	48.4-55.7	52 ± 3
	mole% CO_2		16.2-25.8	21 ± 2	17.3-21.5	20 ± 2
	T_H (CO_2) to liquid		303.5-304.3	303.9 ± 0.2		
	T_H (CO_2-H_2O) to gas		574.2-577.6	576.1 ± 0.8		

growth imperfections exist along the healed crack (Fig. 4),
such as dislocation arrays and solid inclusions (presumably
from silver oxalate). The dislocation arrays represent a stress
field around the dislocation line with an established Burgers
vector parallel to $\langle a \rangle$. The dislocations may be connected to
the inclusions as illustrated in Fig. 5.

The initially introduced cracks in core 6 were investigated
morphologically by the SEM before experimentation. Their
shapes (Fig. 6) vary from smooth curved planes without ir-

regularities to planes with various steps, which are often ar-
ranged in feather-like patterns. After E421, observations were
made of newly grown quartz in the cracks as shown in Fig.
7a. The saw-tooth pattern on one side of the smooth curved
crack represents the newly grown quartz. The orientation
and regularity of the sides of the saw-tooth pattern indicate
a crystallographically controlled overgrowth. Quartz over-
growth on a crack surface, oriented approximately parallel
to the basal plane of quartz is illustrated in Fig. 7b, revealing

Table 3.

Averages and standard deviations of homogenization temperatures
(in Kelvin) from CO_2 and CO_2-H_2O gas mixture of fi.s, before (E679)
and after re-equilibration (V1 and V4).

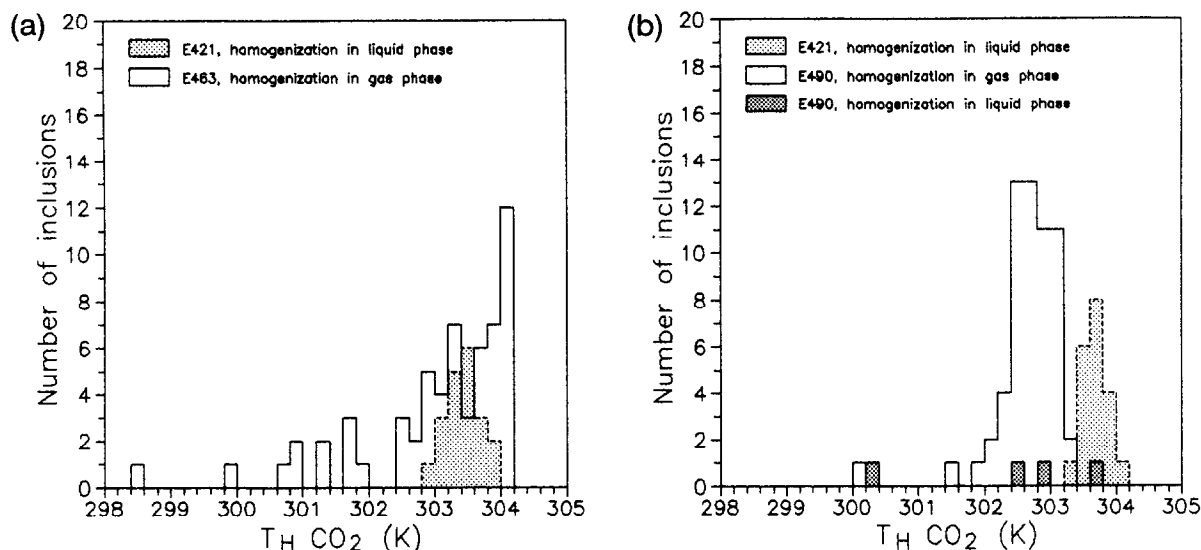|	core	T_H (CO_2) to gas phase	T_H (CO_2-H_2O) to gas phase
E679	1,2	302.17 ± 0.06	573.6 ± 0.4
V1	1	302.22 ± 0.07	573.3 ± 0.7
V4	2	301.95 ± 0.25	575.0 ± 0.8

FIG. 2. Histograms of CO_2 homogenization temperatures (T_H CO_2) of fi.s in quartz cores 3 and 4 used in the initial experiment E421 and the corresponding re-equilibration experiments E463 (a) and E490 (b). Only type 2 fi.s are considered (see text).

growth-hillocks consisting of flat regions between microsteps. Channels and inclusions are developed at irregularities on the surface of the quartz, at sites where no quartz growth has occurred. The channels are of the same order of magnitude as those determined by TEM (Fig. 4), varying between 0.05 and 0.2 μm. The morphologies of the inclusion walls were examined. An opened inclusion of approximately 20 μm diameter is seen in Fig. 8. Four pits (about 0.5 μm diameter) on the inclusion wall are shown at the bottom left; these are assumed to be openings of some channels.

Test Experiments V1 and V4

Two extra runs were carried out to test the effectiveness of the experimental method. In both experiments (V1 and V4), no brittle failure in the quartz around the inclusions was observed after the runs. Only T_H was used as a measure of possible changes of density and compositions, as the errors in T_H measurements are smaller than those in volumetric determinations. The volumetric proportions of the phases did not change. For both experiments, no significant changes occurred in T_H (Table 3). This indicates that the observed changes in the re-equilibration experiments E463 and E490 did occur at the desired pressure and temperature.

Re-Equilibration for Isothermal Decompression in E463

Quartz core 3 was pressurized at 100 MPa (Table 1). At 835 K, an overpressure of approximately 100 MPa was created in the original H_2O-CO_2 inclusions. Fig. 3a gives all measured T_H. The T_H of fi.s illustrated in Fig. 9 are listed in Table 4. Two distinctive types of inclusions were recognized in the core:

1) *Type 1 fi.s* start to form during renewed healing of cracks which were only partly healed in initial experiments. Two-phase pure H_2O inclusions (Fig. 9a) homogenize to the liquid phase at an average temperature of 646 K. A minority of type 1 inclusions consist of water with variable

low mole fractions CO_2, displaying two- and three-phase inclusions, respectively. The H_2O and CO_2 phases homogenize to the liquid phase at high temperatures and to the gas phase at low temperatures between 584.8 and 651.4 K.

2) *Type 2 fi.s* are re-equilibrated original inclusions. This alteration is marked by major changes in composition and minor changes in inclusion shape. The solution and precipitation of the irregularly shaped inclusion walls may locally produce more rounded forms. The CO_2 phases homogenize to the gas phase at temperatures ranging from 298.5 to 304.2 K (Fig. 2a), which is evidently lower than for the initial inclusions of E421. The volume percentage CO_2 (liquid and vapor) values for examples given in Fig. 9b, c, and d correspond with Table 4. All measured values vary between 60 to 92; these present an increase with respect to those of E421. The H_2O and CO_2 phases homogenize to the gas phase between 571.5 and 608.2 K (Fig. 3a). At the edge of the quartz core, inclusions were observed containing only CO_2 with extremely low T_H (280 K, not represented in Fig. 3a). The decrease in density of the CO_2, independent of the amount of decrease, corresponds to the increase in partial volume of CO_2, due to the loss of H_2O in the inclusions. Some inclusions show evidence of decrepitation (newly formed micro-cracks, Fig. 9d), without loss of the included gas mixture. No CH_4 or CO was detected with Raman microscopy after the experiment.

Re-Equilibration for Isothermal Compression in E490

The quartz core was repressurized to 365 MPa (Table 1). At 835 K an underpressure of about 165 MPa was created within the original fi.s. All measured T_H are shown in Fig. 3b. For example, the T_H of inclusions in Fig. 10 yields two values related to different types of fi.s (Table 4):

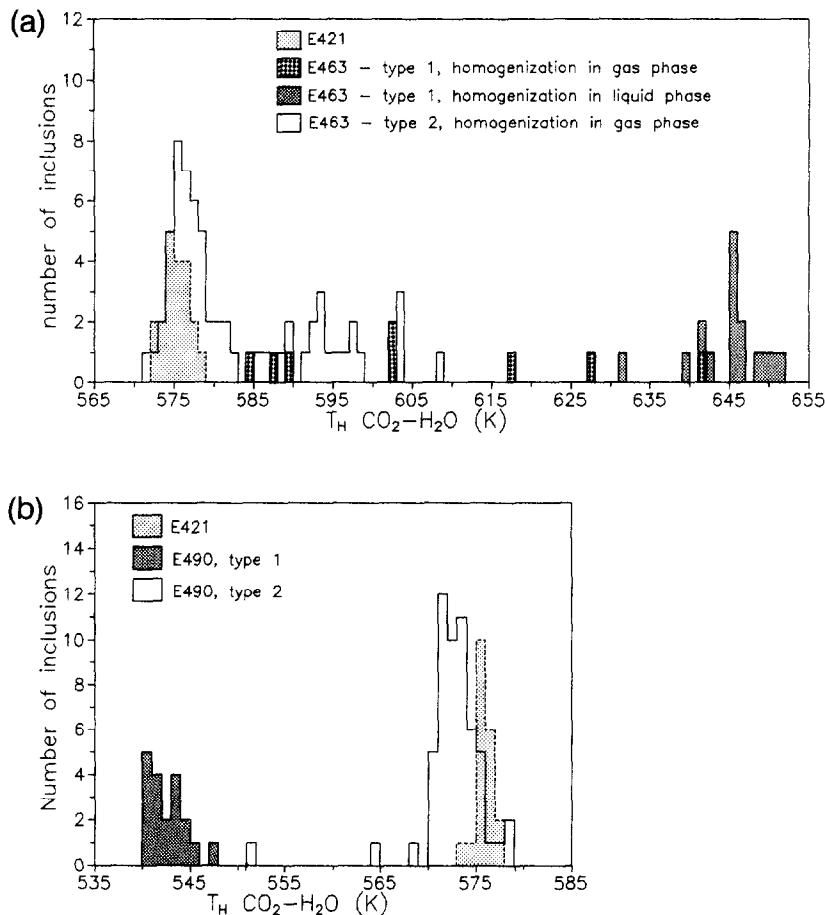1) *Type 1 fi.s* (Fig. 10a) are newly generated in E490. The average volume occupied by the gas bubble is about 24%

FIG. 3. Histograms of CO_2-H_2O homogenization temperatures (T_H CO_2-H_2O) from fi.s in quartz cores 3 and 4 used in the initial experiment E421 and the corresponding re-equilibration experiments E463 (a) and E490 (b). All measured type 1 and 2 fi.s are represented in the histograms.

of the total volume at 293 K. The fi.s homogenize to the liquid phase at temperatures ranging from 540.7 to 548.0 K, with a frequency peak at 541 K (Fig. 3b).

2) *Type 2 fi.s* are re-equilibrated original fluid inclusions. No sign of decrepitation around the fi.s was observed. Solution and precipitation of quartz, which has occurred at the walls of the inclusions (Fig. 10b and c), was more pronounced than in E463. The gas bubble volume increase is clearly illustrated in Fig. 10b and c. The volume percentage CO_2 (liquid and vapor) in the re-equilibrated inclusions ranges from 38 to 80% of the total volume (some examples are given in Table 4). The CO_2 phases homogenize between 300.3 K to the liquid phase and 300.1 K to the gas phase (Fig. 2b). The CO_2 and H_2O phases homogenize to the gas phase at temperatures ranging from 551.4 to 579.3 K, with a frequency peak at 572 K (Fig. 3b). Again no CH_4 or CO was detected with Raman microscopy after the experiment.

Summarizing, in both re-equilibration experiments the type 2 fi.s have reduced densities and increased mole fractions of CO_2. From these results we must assume H_2O leakage. Any fluid leakage by decrepitation is reasonable for E463 as the fluid in the inclusions has an overpressure. However, the observed leakage of H_2O from E490 was unexpected, as it was

presumed that the underpressure would lead to H_2O infiltration.

DISCUSSION

STERNER and BODNAR (1989) reported a density increase in fluid inclusions re-equilibrated at internal underpressure conditions, whereas PECHER (1981) described a density decrease. BAKKER and JANSEN (1990) observed an unexpected density decrease for experiments simulating isobaric cooling. Our new experiments argue for density decreases during re-equilibration with both internal under- and overpressure.

Using mechanisms for inclusion re-equilibration such as those suggested by STERNER and BODNAR (1989), we initially expected changes of volume without any significant leakage of H_2O or CO_2. We expected that the volume of individual inclusions in E463 and E490 should have been increased by 146% and reduced by 74% of the original volume, respectively. However, the microphotographs from both experiments (Figs. 9 and 10) reveal only minor volume changes. The estimated X_{CO_2} values (Table 4) indicate a loss of H_2O from the fluid inclusions during re-equilibration.

The calculated X_{CO_2} from flat fi.s, after the initial experiment E421 is higher than the value calculated from the amounts silver-oxalate and water (Table 1). This discrepancy

FIG. 4. A composite of a series of bright field electron micrographs, revealing a healed microcrack of about 10 μm thickness in core 1 after E421. The synthetic fi.s (white spots) of around 1 to 2 μm radius, end in long (visible a maximum of 15 μm), narrow (about 0.1 μm diameter) channels (white curved lines). Between the fi.s, incorporated particles and dislocation arrays (dark curved lines) are visible. The phenomena are sketched schematically, bottom-left side. The position of the healed crack is indicated by the stippled line. The white square is enlarged in the top-right corner, revealing dislocation arrays visible for more than 1 μm in length.

may result from impurities in the silver-oxalate or loss of substances during welding of the gold-tubes. The density calculated for the experimental conditions of E421 using the equation of state, described by CHRISTOFORAKIS and FRANCK, 1986 (CF-equation) is 21.6 mmol/cm^3. The fluid density in the inclusions has been assumed to be equal to the
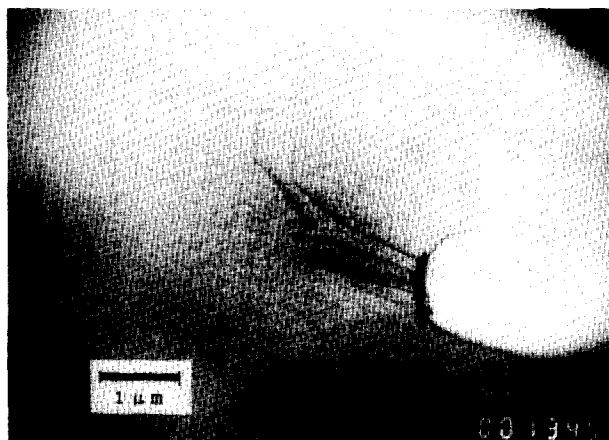
FIG. 5. Bright field electron micrograph (TEM) of a synthetic fluid inclusion (white) of radius 1 μm in core 1 from E421, with a series of 6 pinned dislocations (dark lines) with an average length of 2 μm.

density in the capsule, but the value is too low with respect to the densities, calculated from our volume estimations and solubility tables, of 34.7 and 32.9 mmol/cm^3, respectively, for cores 3 and 4. The theoretically calculated densities have been used to predict the $T_H(H_2O\text{-}CO_2)$, with data from TA-KENOUCHI and KENNEDY (1964) on the miscibility gap in $H_2O\text{-}CO_2$ gas mixtures. The inaccuracy of the equation of state for $H_2O\text{-}CO_2$ mixtures in the vicinity of the miscibility gap does not permit exact prediction of T_H.

Type 1 Fluid Inclusions

Type 1 fi.s were expected to contain pure H_2O. The fluids have a density 23.9 ± 0.4 mmol/cm^3 and 42.3 ± 0.5 mmol/cm^3 (CF-equation) for E463 and E490, respectively. Homogenization should occur at 645 ± 1 and 528 ± 1 K to the liquid phase for E463 and E490, respectively (Fig. 1).

The peak-frequency for T_H in E463 (Fig. 3a) is in accordance with 645 K. The variations in volumetric proportions for E463 may also be attributed to the influx of some CO_2. This CO_2 must originate from original inclusions and is presumed to have migrated along fractures, resulting from the internal overpressure of approximately 100 MPa. The abundant presence of pure H_2O inclusions indicates that the CO_2 source was not available in the beginning of the experiment. The pure water inclusions were probably created in advance of decrepitation of the original CO_2-containing inclusions. By continued decrepitation, the free gas-mixture in the capsule will be progressively enriched with small amounts of CO_2. Evidence for decrepitation in E463 was seen in the form of new microcracks around fi.s (Fig. 9d).

The wide range of T_H in E490 (Fig. 3b) indicates the existence of small amounts of CO_2 in the water phase. Although no signs of decrepitation or implosion are observed in E490, a similar process must have affected the T_H of type 1 inclusions, resulting in a range of elevated temperatures (Fig. 3).

Type 2 Fluid Inclusions

When pressure-equilibrium is approached for the same $H_2O\text{-}CO_2$ gas-mixture in re-equilibration experiments as in

the initial experiment, the theoretical fluid-density for E463 should decrease (15.7 mmol/cm^3, CF-equation) and for E490 should increase (27.8 mmol/cm^3, CF-equation). The T_H for E421 of 575 K, calculated using the CF-equation, is in accordance with the measured value of 576.1 and 575.6 K, respectively, for cores 3 and 4. T_H, derived from our density calculation, is about 515 K.

Using available $P\text{-}V\text{-}T\text{-}X$ data for the system $H_2O\text{-}CO_2$, it is possible to predict T_H of re-equilibrated fi.s with constant volume assuming four different models of re-equilibration (Fig. 11):

1) Leakage of a $H_2O\text{-}CO_2$ gas mixture with composition 19 ± 3 mol% CO_2 for E463 (Fig. 11a) will keep the mole fractions constant. The position of the miscibility gap within the $P\text{-}T$ field will then remain unchanged. Depending on the amount of leakage, T_H will lie between 575 K and a maximum of 613 K. Infiltration of the involved gas mixture for E490 was not possible, as only H_2O was available outside the quartz core.

2) Preferential leakage of H_2O in E463 will produce an enrichment of CO_2 (Fig. 11b) and will instantaneously lead to an increase of T_H to a maximum of 603 K, followed by a decrease until pressure-equilibrium is reached, at 33 mol% CO_2 and 577 K.

3) Infiltration of H_2O for E490 will produce a low X_{CO_2} (Fig. 11c). T_H will vary between 575 and 539 K, depending on the amount of infiltration until pressure-equilibrium is reached at 16 mol% CO_2.

4) As described by BAKKER and JANSEN (1990), leakage of fluid may occur under conditions of internal underpressure. Therefore, preferential leakage of H_2O and leakage of 21 ± 2 mol% CO_2 gas mixture are considered for E490. The effects on T_H are similar to those described in 1) and 2) above.

Despite the large errors, volume estimations indicate the leakage of H_2O from some inclusions (Table 4). The change

FIG. 6. SEM photomicrographs of crack surfaces, created by quenching the quartz core 2 in water after heat treatment at 623 K before the original experiment E421. The morphology varies between smooth curved planes and a feather-like pattern of small steps.

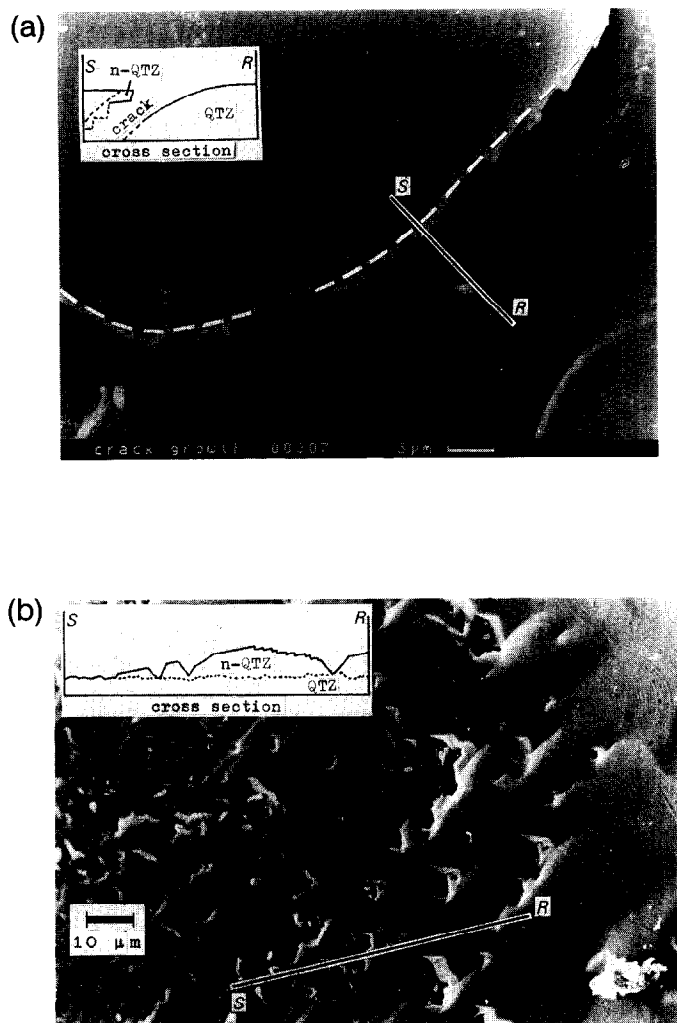FIG. 7. (a) SEM photomicrograph of crystal growth along a crack of about 2 μm thickness in core 2 after E421. The plane of projection is tilted 10 degrees from the basal plane, about a rotation axis approximately parallel to the a-axis. Quartz overgrowth, only on the upper quartz surface below the dashed line (marking the original crack surface), occurs in regular patterns, defined by crystallographical orientations (see text). (b) SEM photomicrograph of crystal growth on a crack surface in core 2, showing growth-hillocks which are similarly defined by crystallographical orientations, with flat regions between the macrosteps of about 1 μm. Imperfections inherited from irregular growth, which is presumably initiated on small quartz particles and or defects on the crack surface, are the instigators for long, narrow channels, illustrated in Fig. 4 (QTZ = quartz, n-QTZ = newly grown quartz).

in T_H due to leakage of gas mixtures or individual gas species is in accordance with the experimentally determined trend (Fig. 12). The data from E490 (Fig. 12b) suggest that model 3 is not operating.

A theoretical curve, using the CF-equation, for type 2 fi.s giving the relationship between T_H and mol% CO_2, based on preferential leakage of H_2O, is superimposed on Fig. 12 (Curve 3). The derived best fit through our data (Fig. 12, curves 1 and 2 for E463 and E490, respectively) does not match the theoretical curve 3. Theoretical curve 4 with initial lower densities (17 mmol/cm³) and higher mole fractions

CO_2 (35%), plots the nearest to our best-fit curves 1 and 2. STERNER and BODNAR (1991) have shown that the solved data of TAKENOUCHI and KENNEDY (1964) are probably in error. However, the differences do not affect the trend in T_H changes. Therefore, the large error possible in volume estimations, inaccuracy of the CF-equation, or extreme non-ideal mixing behaviour of H_2O and CO_2 near the miscibility gap may result in deviations from the calculated theoretical curve.

The data from E463 (Fig. 12a) having relatively high T_H and low mol% CO_2 values can be explained by micro-cracking around fi.s due to the internal overpressure (Fig. 9d). This volume increase causes data from curve 1 to shift to higher T_H, while the mol% CO_2 remains constant. Volume decrease for E490 (Fig. 12b) at constant mol% CO_2 causes T_H to shift to lower values. It is suggested that the large amount of solution and precipitation at the walls of the fi.s in E490 (Fig. 10b and c) is evidence of this volume decrease.

The amount of gas leakage, evident in most fi.s (Figs. 9b, c, and 10 b, c), cannot be accounted for by optically observed features. Four mechanisms of fluid leakage during experimentation may be evaluated.

Point defects

Diffusion of H_2O via point defects through quartz may contribute to leakage from fluid inclusions. The mobility of water species through quartz was proved by the determination of water concentrations in bubbles in synthetic quartz after heating to 1173 K at 300 MPa (BALDERMAN 1974; PATERSON and KEKULAWALA, 1979; MCLAREN et al., 1983).

Estimations of the bulk-diffusion coefficient vary between 10^{-10} at 1273 K (BLACIC, 1981; KRONENBERG et al., 1986) and 10^{-23} m²/s at 773 K (DENNIS, 1984), depending on the diffusing species (O, H, OH, or H_2O), direction of diffusion, and experimental conditions.

Taking into account our experimental conditions, the diffusion coefficient is likely to be in the order of 10^{-23} m²/s. The transport distance, roughly expressed by the term $(Dt)^{1/2}$ (FLETCHER and HOFMANN, 1974), is 1.5 nm during the experiment. Assuming the water solubility in quartz to
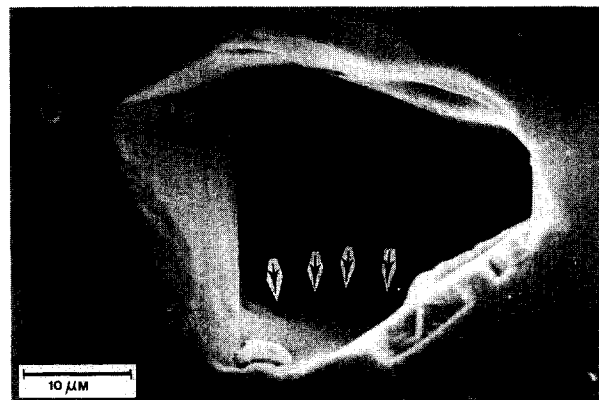

FIG. 8. SEM photomicrograph of an opened inclusion (radius 10 μm) in core 2, revealing a series of four small channels with radii of about 0.5 μm, on the inclusion wall (arrows left down), as was visualized with TEM (Fig. 4).
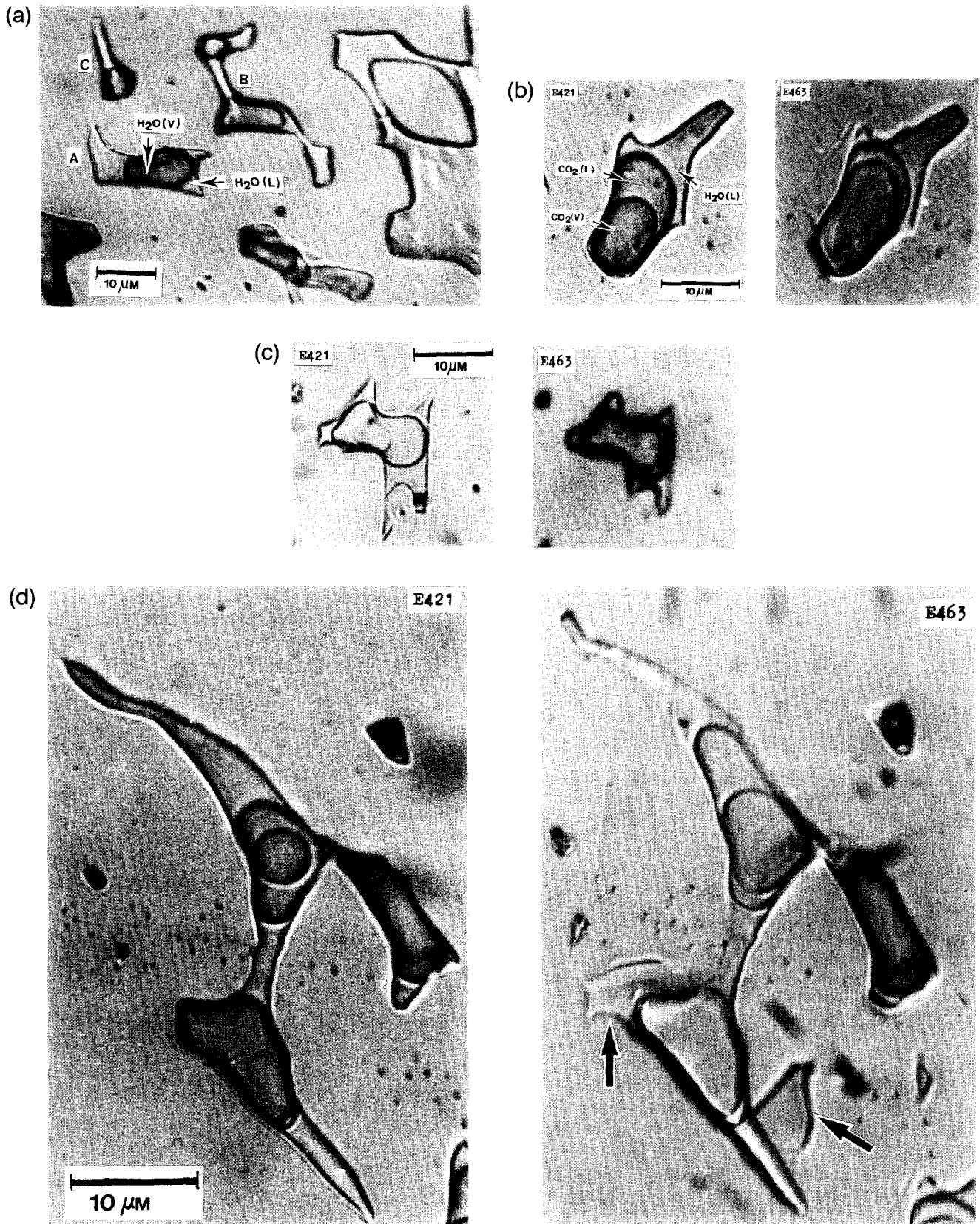
FIG. 9. Photomicrographs of fluid inclusions before (E421) and after (E463) re-equilibration at 100 MPa and 835 K in core 3. The various phases, CO_2 (liquid and vapor) and H_2O (liquid and vapor) are indicated. (a) Type 1 fi.s containing pure H_2O which are representative of new hydrothermal conditions after E463. (b and c) Type 2 fi.s compared to the original inclusions after E421. (d) Type 2 fi. with newly grown microcracks (arrows) after E463.

Table 4.

Optically estimated volumetric percentages of CO_2 and H_2O phases, mole

percentages CO_2 and T_H of CO_2, of CO_2-H_2O mixture and of H_2O in a few selected type

1 and 2 fi.s from the quartz cores after E463 and E490, corresponding to the

illustrated re-equilibrated fi.s in photomicrographs in figures 9 and 10.

Homogenization in liquid (l) or gas (g) phase is indicated in the headings of

the table.

fluid inclusion			volume percentages				mol% CO_2	homogenization temperatures (Kelvin)		
			CO_2		H_2O					
exp.	fig.	type						CO_2 (g)	CO_2-H_2O (g)	H_2O (l)
			vap.	liq.	vap.	liq.				
E 463	9A	A:1	–	–	49	51	–	–	–	650.0
		B:1	–	–	52	48	–	–	–	650.3
		C:1	–	–	55	45	–	–	–	650.8
	9B	2	48	24	–	28	33	304.0	591.8	–
	9C	2	56	24	–	20	38	303.5	579.4	–
	9D	2	48	22	–	30	28	304.1	593.5	–
E 490	10A	1	–	–	23	77	–	–	–	546.2
	10B	2	50	18	–	32	23	302.5	571.1	–
	10C	2	58	20	–	22	26	301.8	572.8	–

be 100 H/10^6 Si, an inclusion of radius 5 μm would only lose 5 × 10^{-7} mol% H_2O. Therefore, diffusion by point defects is too slow to be effective in leakage of H_2O from the inclusions within the experimental time.

Dislocations

Diffusion of water species through dislocations in quartz was elucidated by ROEDDER and SKINNER (1968), GRIGGS (1974), MCLAREN et al. (1983), DOUKHAN and TREPIED (1985), and HOLLISTER (1989). Dislocations should not be considered as open channels in the quartz crystal through which H_2O and CO_2 can leak or infiltrate by capillary flow, but as distortions of the crystal lattice on a nanometer scale. However, H_2O and CO_2 are likely to diffuse faster through the crystal along dislocation cores, where there is more space for movements, than through a system of point defects. The pipe diffusion coefficient (YUND et al., 1981) can be five orders of magnitude larger than the bulk diffusion coefficient by point defects. Fi.s connected to dislocation loops, as described by MCLAREN et al. (1983) and DOUKHAN and TREPIED (1985), are observed in our experiments (Fig. 5). Mobile dislocations discontinously tapping fi.s may become saturated with water and carry small amounts from the inclusions through the quartz crystal. Furthermore, fi.s are principally major imperfections and may act as sources for dislocation multiplication. Deviatoric stress states around fi.s, caused by the internal over- or underpressure may stimulate mobility

of dislocations. Preferential H_2O leakage may result from both physical and chemical interaction between the hydrophilic quartz surface and the water dipoles, causing local immiscibility at the fi walls and in dislocation cores. Even at experimental re-equilibration conditions, the fi. walls may be coated by a molecular film of H_2O. This prevents CO_2 molecules from escaping from the fi.s through routes available at these walls. H_2O loss is a result of enhanced solution of H_2O with respect to CO_2 in and around the dislocation core. The exact process by which fractionation may occur could involve diffusion controlled fractionation due to different molecular sizes.

If a dislocation is saturated with H_2O, the stress potential cloud, visible using the TEM (Fig. 5), contains 50–100 times as many H_2O molecules as are bound in the dislocation core (edge of the half plane; GRIGGS, 1974). Assuming that dislocations have an average length of 1 mm and a core radius between 0.25 (YUND et al., 1981) and 1 nm (HIRTH and LOTHE, 1968), and that they are connected with fi.s, under internal overpressure, they will become saturated with H_2O. We calculated that about 33 mobile dislocations have to pass a H_2O-rich inclusion of radius 5 μm in order to lose 20 mol% of its contents.

Channels

In Fig. 7a, crystal growth along the crack is irregular. This growth is dependent on the crack wall morphology and
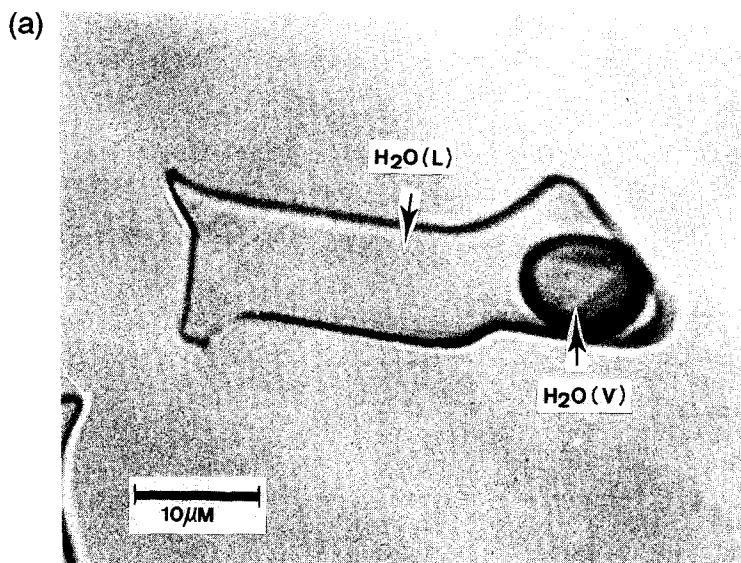
(a)

FIG. 10. Photomicrographs of fluid inclusions before (E421) and after (E490) re-equilibration at 365 MPa and 835 K. The various phases, CO_2 (liquid and vapor) and H_2O (liquid and vapor) are indicated. (a) Type 1 fi. containing pure H_2O which is representative of new hydrothermal conditions. (b and c) Type 2 fi.s compared to the original inclusions after E421. Solution and precipitation of quartz on the fi. walls transformed the rim, creating irregularities.

experimental conditions. As our photographs (Fig. 4) reveal, crack healing processes do not restore the quartz to a perfect crystal. In addition to many built-in defects, small channels with a maximum diameter of 0.1 μm (Fig. 4), which are optically invisible, are the only remaining portions of the crack. The observed fi.s are connected to a maximum of 10 channels (Fig. 8 reveals only 4 channels). In E463, with an over-pressure gradient of 100 MPa, capillary flow through these channels may be an effective mechanism for fluid transport. H_2O-CO_2 fluids in pores with diameters less than 2.5 nm differ in composition (richer in H_2O) from the bulk fluid in the inclusion (BELONOSHKO, 1989). Therefore, local immiscibility of H_2O-CO_2 gas-mixtures may occur even at PT conditions outside those for the determined miscibility gap. Fluids in small channels may differ in composition from fluids in the larger inclusions. Capillary fluid separation (WATSON and BRENAN, 1987; YARDLEY and BOTTRELL, 1988), which is effective within the miscibility gap at low PT conditions, may also cause preferential leakage of H_2O at conditions of presumed total miscibility. For E490, infiltration of H_2O was expected due to the existence of a reversed pressure gradient; this was not observed. At room conditions, transport by capillary flow of fluid out of the inclusions from both experiments E463 and E490 is to be expected, due to the internal pressure of about 4 MPa if the channels are connected to the surface of the core. However, the fi.s do not seem to change in composition or density after the experiments.

Cracks

The importance of cracks developed during experimentation was pointed out by several authors (PECHER, 1981; GRIGGS, 1974; DEN BROK and SPIERS, 1991; KRONENBERG et al., 1986; GERRETSEN et al., 1989). They emphasize the importance of extensive microcracking as a mechanism by which molecular water may enter quartz, in addition to a mechanism of dislocation slip during deformation experiments. We observed newly developed cracks only in experiment E463. Preferential leakage would occur, if the thickness of the cracks were less than 2.5 nm (BELONOSKHO, 1989), in the same manner as previously described above for channels. These nano-cracks are too small to be visible with an optical microscope and were not observed with SEM.

GEOLOGICAL APPLICATION OF OUR EXPERIMENTS

Natural fi.s in Metamorphic Quartz

The processes of cracking and crack-healing within quartz grains occur often during the deformation of metamorphic rocks and are evidenced by trails of fi.s. Assuming the natural crack-healing process to be principally similar to our experimental process, preferential leakage of H_2O out of initially H_2O-rich inclusions may occur during uplift and cooling. We expect the leakage mechanisms that have operated during our short experimental runs, and have already been discussed, to be more effective in real geological processes. TEM-photomicrographs of natural fi.s often reveal dislocations connected to inclusions. Primary fi.s change in density and composition, the amount of change being dependent on the extent of deformation, due to H_2O transport by means of dislocations and imperfections or through channels and nano-cracks.

Isothermal Decompression (as Exemplified by the Rocks on Naxos, Greece)

The main part of the island of Naxos consists of a metamorphic complex of alternating schists and marbles surrounding a central migmatite dome. The peak-metamorphic grade generally increases towards the dome. Fi.s in quartz
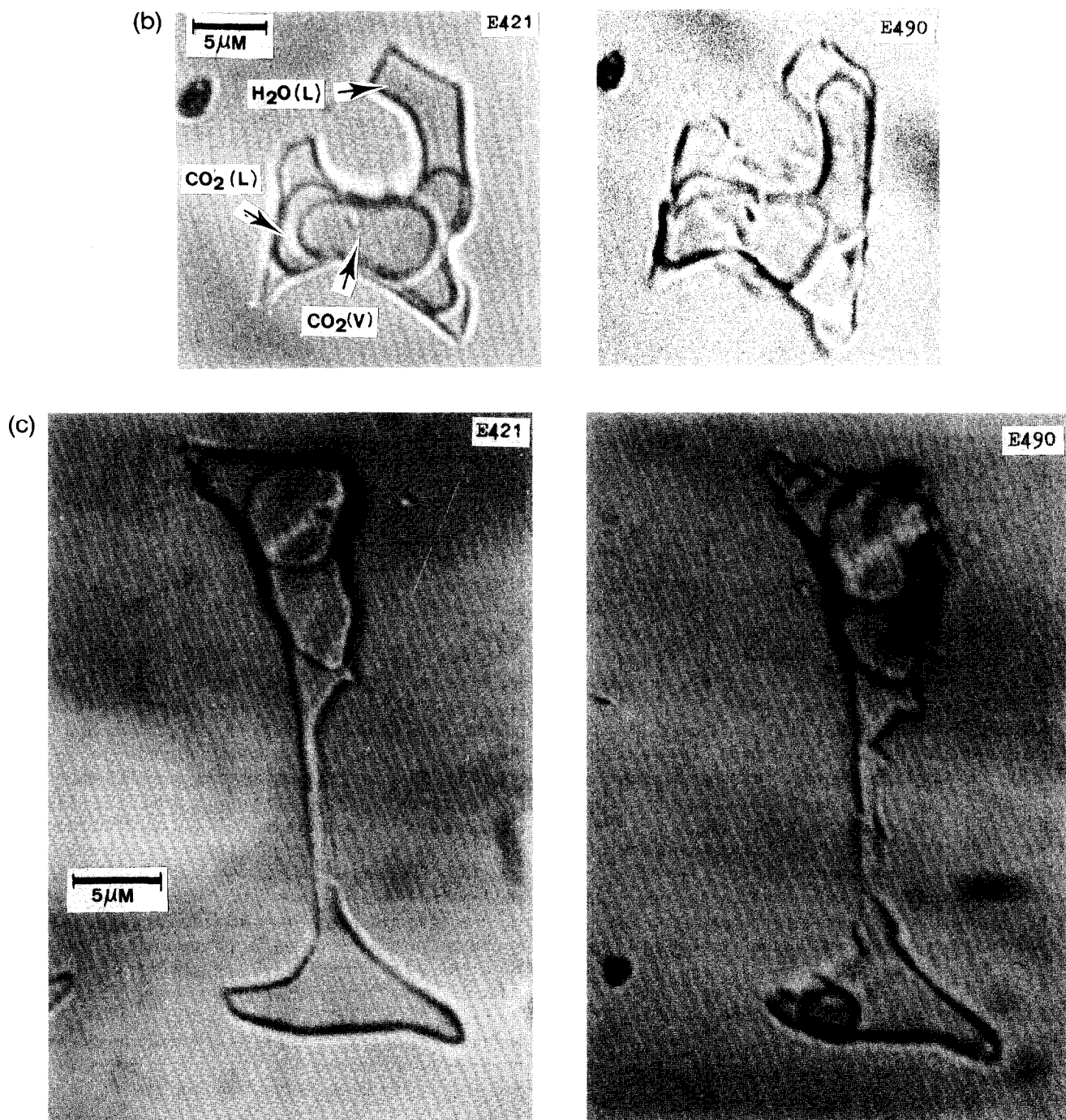
FIG. 10 (Continued)

lenses from Naxos have been investigated extensively by KREULEN (1977, 1980), and he suggested that they are predominantly CO_2-rich with minor amounts of H_2O. The composition of the optically studied fi.s seemed to be independent of metamorphic grade and lithology, in contradiction to the mineral reaction path buffered by the siliceous dolomites (JANSEN et al., 1978). Fi.s contain 60–90 mol% CO_2 from optical estimates (KREULEN, 1980). However, collecting gasses in a vacuum line after decrepitation of the fi.s, resulted in 6–91 mol% CO_2 (KREULEN, 1977).

At the end of the main metamorphism, there was a considerable drop in P_{total} of at least 300 MPa (JANSEN et al., 1977, BUICK and HOLLAND, 1989) accompanied by an extensional penetrative deformation (LISTER et al., 1984; URAI et al., 1989) with corresponding folding (PAPANIKOLAOU, 1986) and the resetting of isogrades towards the center of the dome (JANSEN et al., 1989). Of course, the final fluid densities in the inclusions are much lower than those expected for peak-metamorphic conditions, calculated from petrological and geothermometrical data. Practically all water-rich
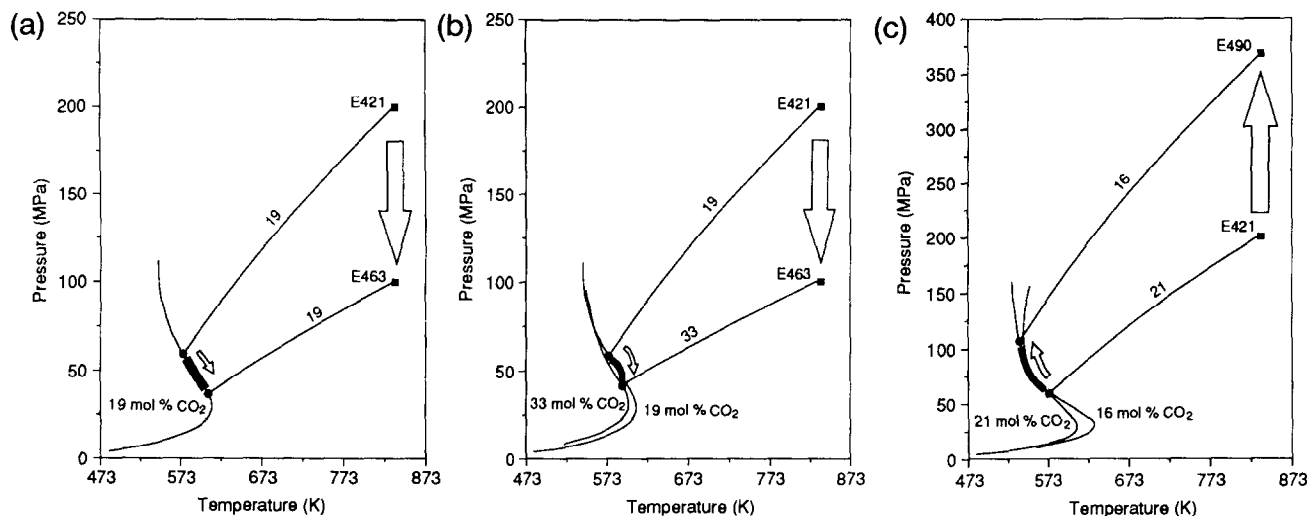
FIG. 11. Models for the change in T_H in E463 and E490. Isothermal compression and decompression are indicated with large arrows. The small arrows indicate the corresponding PT-path of homogenization conditions. (a) Leakage of 19 mole% CO_2 gas mixture in E463. (b) Preferential leakage of H_2O in E463. (c) Infiltration of H_2O in E490. The models are further explained in text.

inclusions must have leaked selectively or decrepitated during the pressure-drop. Fi.s were exhumed, resulting in a more CO_2-rich composition, while small H_2O-rich fi.s developed in the newly grown micro-cracks caused by decrepitation. There exists a positive correlation between X_{CO_2} and the size of the fi.s (F. POSTMA, pers. comm. 1990).

The optically established X_{CO_2} in the inclusions (KREULEN, 1980) is much too high for various mineral assemblages. For example, the occurrence of epidote minerals requires that CO_2 content of the metamorphic fluid did not exceed 10 mol% (JANSEN and SCHUILING, 1976; JANSEN et al., 1989; BAKER et al., 1989). The post-peak metamorphic P-T path approaches an isothermal decompression. Therefore, the anomalous values for the densities and compositions of fi.s from Naxos can be explained by comparison with the observed changes in the isothermal decompression experiment E463.

Isobaric Cooling (as Exemplified by the Rocks on Rogaland, Southwestern Norway)

SWANENBERG (1980) conducted an extensive study of fi.s in rocks from Rogaland, Norway. Here are found anorthosite complexes, a lopolith of monzonoritic to noritic composition with its surrounding high grade metamorphic envelope. JANSEN et al. (1985) and MAIJER and PADGET (1987) have recognized three Proterozoic metamorphic episodes: M1, old regional metamorphism; M2, peak granulite facies metamorphism resulting from the thermal event associated with the intrusive masses; M3, the widespread introduction of fluid during regional cooling (decomposition of M2 minerals). The gaseous fi.s have wide ranging compositions (VAN DEN KERKHOF et al., 1991; SWANENBERG, 1980) within the CO_2, CH_4, and N_2 triangle.

There are many discrepancies between the metamorphic P-T path derived from the mineral assemblages of Rogaland and the isochores of the measured densities and compositions

of fi.s. Firstly, there are metastable mixtures of CO_2 and CH_4; and secondly, both low and extremely high densities are observed.

The gas mixture CO_2-CH_4 is chemically unstable and should react to H_2O and graphite, until H_2O makes up approximately 80 mol% of the fluid. A metastable CO_2-CH_4 mixture may remain after preferential water leakage if the threshold energy for their reaction is too high.

Low densities cannot be explained by recrystallization of the quartz, which occurred at conditions of higher densities. However, these low densities can be explained by assuming partial leakage of gasses. This phenomenon was observed in experiment E490 and is also described previously by BAKKER and JANSEN (1990). High density CO_2 inclusions result from the post entrapment re-equilibration of pre-existing inclusions towards the higher densities reached by near isobaric cooling (SWANENBERG, 1980; VAN DEN KERKHOF et al., 1991). However, several high densities are out of range of the post metamorphic trajectory. VAN DEN KERKHOF et al. (1991) propose formation of inclusions at very low temperatures. We propose simultaneously operating mechanisms of post-peak metamorphic re-equilibration and volume adjustments, leading to the very high density inclusions.

CONCLUSIONS

1) In hydrothermal recrystallization experiments with quartz containing H_2O-CO_2 fi.s with 19 and 21 mol% CO_2, density decreases are obtained under near-constant volume conditions by both preferential leakage of H_2O and leakage of the gas mixture.

2) Preferential leakage of H_2O occurred in experiments which simulated both isothermal decompression (E463) and isothermal compression (E490), despite the reversed pressure and water fugacity gradient in E490.

3) Leakage of H_2O must have proceeded by diffusion along mobile dislocation lines, while point defect diffusion can-
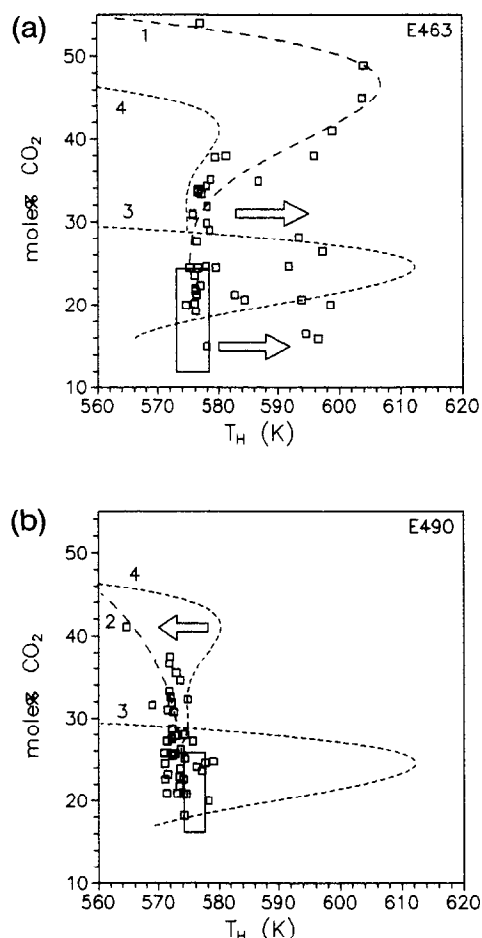
FIG. 12. T_H-X_{CO_2} diagrams for type 2 fi.s of E463 (a) and E490 (b). All data from the original experiment E421 lie within the large rectangles. Data of the re-equilibration experiments are indicated by small squares. Dashed curves 1 and 2 are best-fits through the data from E463 and E490, respectively. Dashed curve 3 is the theoretically H_2O-leakage relation between T_H and X_{CO_2} based on the initial 17.8 mol% CO_2, the CF-equation of state, and the experimentally derived miscibility gap for the H_2O-CO_2 gas-mixture (TAKENOUCHI and KENNEDY, 1964). Dashed curve 4 is a curve based on the same theory with an initial mol% CO_2 of 35%, which seems to fall between and fit best the main data points of both diagrams. The horizontal arrows indicate the effect on T_H for E463 and E490 due to volume increase and volume decrease, respectively. Notice the decrepitation in E463 (also Fig. 9d).

not be responsible for the amount of leakage involved. The high density of defects within the healed crack, as established by TEM work, may indicate that the former crack as a whole may have provided an important route for the leakage for gas species out of the inclusions.

4) We propose that re-equilibration as described in our experiment would be effective in metamorphic quartz, during cooling and uplift.

5) In natural rocks, fi.s are often assigned to several generations of fluid with variable compositions, leading to the assumption of an extensive variety of metamorphic fluids, that may have passed through the vein. These experiments clarify that a wide compositional range of fi.s can be generated from a single type of fi. by H_2O-leakage initiated

by local recrystallization, which is not necessarily uniform, even in an individual healed crack.

6) Metamorphic conditions obtained by isochore-extrapolation and intersection are nonrealistic when information regarding quartz recrystallization and from valid geothermometry and geobarometry on coeval mineral assemblages is lacking.

7) CO_2-rich fi.s which are claimed for most high-grade rocks have not necessarily always been CO_2 rich, but might have contained high quantities of H_2O.

8) The supposed trend that deep rocks, such as granulites and mantle rocks, contain more CO_2 than H_2O in fi.s may partly be caused by the fact that before exposure, these deep rocks have usually suffered more intensive recrystallization during uplift than shallow rocks.

REFERENCES

ANDRIESSEN P. A. M. (1978) Isotopic age relations within the polymetamorphic complex of the island of Naxos (Cyclades, Greece). Ph.D. thesis, Verh. ZWO-Laboratorium voor Isotopen-Geologie, Amsterdam.

BAKER J., BICKLE M. J., BUICK I. S., HOLLAND T. J. B., and MATTHEWS A. (1989) Isopotic and petrological evidence for the infiltration of water-rich fluids during the Miocene M2 metamorphism on Naxos, Greece. *Geochim. Cosmochim. Acta* **53**, 2037–2050.

BAKKER R. J. and JANSEN J. B. H. (1989) Experimental evidence for leakage of H_2O from CO_2-H_2O rich fluid inclusion. *Terra Abstr. EUG V Strasbourg* **1**, 320.

BAKKER R. J. and JANSEN J. B. H. (1990) Preferential water leakage from fluid inclusions by means of mobile dislocations. *Nature* **345**, 58–60.

BALDERMAN M. A. (1974) The effect of strain rate and temperature on the yield point of hydrolytically weakened synthetic quartz. *J. Geophys. Res.* **79**, 1647–1652.

BELONOSHKO A. B. (1989) The thermodynamics of the aqueous carbon dioxide fluid within thin pores. *Geochim. Cosmochim. Acta* **53**, 2581–2590.

BLACIC J. D. (1981) Water diffusion in quartz at high pressure: Tectonic implications. *Geophys. Res. Lett.* **8**, 721–723.

BOULLIER A. M., MICHOT G., PECHER A., and BARRES O. (1989) Diffusion and/or plastic deformation around fluid inclusions in synthetic quartz: New investigations. In *Fluid Movement-Element Transport and the Composition of the Deep Crust* (ed. D. BRIDGWATER); *NATO ASI Series* C **281**, pp. 345–360. Kluwer Academics Publ.

BUICK I. S. and HOLLAND T. J. B. (1989) The *P*-*T*-*t* path associated with crustal extension, Naxos Cyclades, Greece. In *Evolution of Metamorphic Belts* (eds. J. S. DALY et al.); *Geol. Soc. Spec. Publ.* **43**, pp. 365–369.

BURKE E. A. J. and LUSTENHOUWER W. J. (1987) The application of a multichannel laser raman microprobe (Microdil-28) to the analysis of fluid inclusions. *Chem. Geol.* **61**, 11–17.

CHRISTOFORAKIS M. and FRANCK E. U. (1986) An equation of state for binary fluid mixtures to high temperatures and high pressures. *Ber. Bunsenges. Phys. Chem.* **90**, 780–789.

DEN BROK S. W. J. and SPIERS C. J. (1991) Experimental evidence for water weakening of quartzite by microcracking plus solution-precipitation creep. *J. Geol. Soc. London Bull.* **148**, 541–540.

DENNIS P. F. (1984) Oxygen self-diffusion in quartz under hydrothermal conditions. *J. Geophys. Res.* **89,** 4047-4057.

DODDS W. S., STUTZMAN L. F., and SOLLAMI B. J. (1956) Carbon dioxide solubility in water. *Ind. Eng. Chem.* **1,** 92-95.

DOUKHAN J. C. and TREPIED L. (1985) Plastic deformation of quartz single crystals. *Bull. Mineral.* **108,** 97-123.

FLETCHER R. C. and HOFMANN A. W. (1974) Simple models of diffusion and combined diffusion-infiltration metasomatism. In *Geochemical Transport and Kinetics* (eds. A. W. HOFMANN et al.); *Carnegie Inst. Wash. Publ. 634,* pp. 243-259.

GERRETSEN J., PATERSON M. S., and MCLAREN A. C. (1989) The uptake and solubility of water in quartz at elevated pressure and temperature. *Phys. Chem. Mineral.* **16,** 334-342.

GRATIER J. P. (1982) Approche experimental et naturalle de la deformation des roches par dissolution-cristallisation, avec transfert de matiere. *Bull. Mineral.* **105,** 291-300.

GRATIER J. P. and JENATON L. (1984) Deformation by solution-deposition, and re-equilibration of crystals depending on temperature, internal pressure and stress. *J. Struct. Geol.* **6,** 189-200.

GRIGGS D. (1974) A model of hydrolitic weakening in quartz. *J. Geophys. Res.* **79,** 1653-1661.

HALL D. L., STERNER S. M., and BODNAR R. J. (1989) Experimental evidence for hydrogen diffusion into fluid inclusions in quartz (abstr.). *Geol. Soc. Amer. Abstr. Prog.* **21,** A358.

HIRTH J. P. and LOTHE J. (1968) *Theory of Dislocations,* pp. 780. McGraw-Hill.

HOLLISTER L. S. (1988) On the origin of CO₂-rich fluid inclusions in migmatites. *J. Metam. Geol.* **6,** 467-474.

HOLLISTER L. S. (1989) Enrichment of CO₂ in fluid inclusions in quartz by removal of H₂O during crystal plastic deformation (abstr.). *Geol. Soc. Amer. Abstr. Prog.* **21,** A357.

JANSEN J. B. H. and SCHUILING R. D. (1976) Metamorphism on Naxos: Petrology and geothermal gradients. *Amer. J. Sci.* **276,** 1225-1253.

JANSEN J. B. H., ANDRIESSEN P. A. M., MAIJER C., and SCHUILING R. D. (1977) Changing conditions of Alpine regional metamorphism on Naxos, with special reference to the Al-silicate phase diagram. In *Metamorphism on Naxos* (ed. J. B. H. JANSEN), Ph.D. thesis, Chap. 7, 1-20. State Univ. Utrecht.

JANSEN J. B. H., VAN DER KRAATS A. H., VAN DER RIJST H., and SCHUILING R. D. (1978) Metamorphism of siliceous dolomites at Naxos, Greece. *Contrib. Mineral. Petrol.* **67,** 279-288.

JANSEN J. B. H., BLOK R. J. P., BOS A., and SCHEELING M. (1985) Geothermometry and geobarometry in Rogaland and preliminary results from the Bamble area, S Norway. In *The Deep Proterozoic Crust in the North Atlantic Provinces* (eds. A. C. TOBI and J. L. R. TOURET); *NATO ASI Series C 158,* pp. 499-516. Reidel.

JANSEN J. B. H., VAN DER RIJST H., RYE R. O., ANDRIESEN P. A. M., and RYE D. M. (1989) High integrated fluid rock ratios during metamorphism at Naxos: Evidence from carbon isotopes of calcite in schist and fluid inclusions. *Contrib. Mineral. Petrol.* **103,** 123-126.

KERRICH R. (1976) Some effect of tectonic recrystallization on fluid inclusions in vein quartz. *Contrib. Mineral. Petrol.* **59,** 195-202.

KREULEN R. (1977) CO₂-rich fluids during regional metamorphism on Naxos, a study on fluid inclusions and stable isotopes. Ph.D. thesis, Univ. Utrecht.

KREULEN R. (1980) CO₂-rich fluids during regional metamorphism on Naxos (Greece): Carbon isotopes and fluid inclusions. *Amer. J. Sci.* **280,** 745-771.

KRONENBERG A. K., KIRBY S. H., AINES R. D., and ROSSMAN G. R. (1986) Solubility and diffusional uptake of hydrogen in quartz at high water pressures: Implications for hydrolitic weakening. *J. Geophys. Res.* **91,** 12723-12744.

LISTER G. S., BANGA G., and FEENSTRA A. (1984) Metamorphic core complexes of Cordilleran type in the Cyclades, Aegean Sea, Greece. *Geology* **12,** 221-225.

MAIJER C. and PADGET P. (eds.) (1987) The geology of the southernmost Norway: An excursion guide. *Norwegian Geol. Unders. Spec. Publ.* **1.**

MCLAREN A. C., COOK R. F., HYDE S. T., and TOBIN R. C. (1983) The mechanism of the formation and growth of water bubbles and associated dislocation loops in synthetic quartz. *Phys. Chem. Mineral.* **9,** 79-94.

PAPANIKOLAOU D. J. (1986) Tectonic evolution of the Cycladic Blueschist Belt (Aegean sea, Greece). In *Chemical Transport in Metasomatic Processes* (ed. H. C. HELGESON); *NATO ASI Series C 218,* pp. 429-450. Reidel.

PATERSON M. S. and KEKULAWALA K. R. S. S. (1979) The role of water in quartz deformation. *Bull. Mineral.* **102,** 92-98.

PECHER A. (1981) Experimental decrepitation and re-equilibration of fluid inclusions in synthetic quartz. *Tectonophysics* **78,** 567-583.

PECHER A. and BOUILLIER A. (1984) Evolution a pression et temperature elevees d'inclusion fluides dans un quartz synthetic. *Bull. Mineral.* **107,** 139-153.

ROEDDER E. and SKINNER B. J. (1968) Experimental evidence that fluid inclusions do not leak. *Econ. Geol.* **63,** 715-730.

STERNER S. M. and BODNAR R. J. (1984) Synthetic fluid inclusions in natural quartz 1: Compositional types synthesized and applications to experimental geochemistry. *Geochim. Cosmochim. Acta* **48,** 2659-2668.

STERNER S. M. and BODNAR R. J. (1989) Synthetic fluid inclusions VII: Reequilibration of fluid inclusions in quartz during laboratory simulated metamorphic burial and uplift. *J. Metam. Geol.* **7,** 243-260.

STERNER S. M. and BODNAR R. J. (1991) Synthetic fluid inclusions X: Determination of P-V-T-X properties in the CO₂-H₂O system to 6 kb and 700°C. *Amer. J. Sci.* **291,** 1-54.

SWANENBERG H. E. C. (1980) Fluid inclusions in high-grade metamorphic rocks from S.W. Norway. Ph.D. thesis, *Geol. Ultraiectina* **25,** 1-147.

TAKENOUCHI S. and KENNEDY G. C. (1964) The binary system H₂O-CO₂ at high temperatures and pressures. *Amer. J. Sci.* **262,** 1055-1074.

URAI J. L., JANSEN J. B. H., and SCHUILING R. D. (1989) Deformation in a middle crustal extensional shear zone: An example from Naxos (Greece). *Terra Abstr. EUG V Strasbourg* **1,** 380.

VAN DEN KERKHOF A. M., TOURET J. L. R., MAIJER C., and JANSEN J. B. H. (1991) Retrograde methane-dominated fluid inclusions from high-temperature granulites of Rogaland, southwestern Norway. *Geochim. Cosmochim. Acta* (in press).

WATSON E. B. and BRENAN J. M. (1987) Fluids in the lithosphere, 1. Experimentally determined wetting characteristics of CO₂-H₂O fluids and their application for fluid transport, host-rock physical properties, and fluid inclusion formation. *Earth Planet. Sci. Lett.* **85,** 497-515.

WEAST R. C. (ed.) (1975) *Handbook of Chemistry and Physics.* Table: Physical constants of inorganic components, B 84. CRC Press.

WILKINS R. W. T. and BARKAS J. P. (1978) Fluid inclusions, deformation and metamorphism. *J. Geol. Soc. London* **140,** 657-663.

YARDLEY B. W. D. and BOTTRELL S. M. (1988) Immiscible fluids in metamorphism: Implications of two phase flow for reaction history. *Geology* **16,** 199-202.

YUND R. A., SMITH B. M., and TULLIS J. (1981) Dislocation-assisted diffusion of oxygen in albite. *Phys. Chem. Mineral.* **7,** 185-189.